Depletion of VOC in wastewater by vacuum membrane distillation using a dual-layer membrane: mechanism of mass transfer and selectivity

Depletion of VOC in wastewater by vacuum membrane distillation using a dual-layer membrane: mechanism of mass transfer and selectivity

Jianhua Zhang*[,1], Na Li[2], Derrick Ng[3], Ikechukwu A. Ike[1], Zongli Xie[3], Stephen Gray*[,1]

1. Institute for sustainability and Innovation, College of Engineering and Science, Victoria University, Melbourne, Australia
2. School of Chemical Engineering and Technology, Xi'an Jiaotong University, Xi'an, Shaanxi 710049, P.R. China
3. Manufacturing, CSIRO, Australia

*. Corresponding author

Abstract

In this paper, volatile organic compound (VOC) removal by vacuum membrane distillation with a dual-layer membrane was studied. The mass transfer mechanism and VOC selectivity of the dual-layer membrane for VOC removal were compared with that of the PTFE membrane, for which the separation relied on the liquid-vapour equilibrium of VOCs in water. The VOC mass transfer across the dual-layer membrane could not be completely described by Raoult's law, which is applicable for the performance of the PTFE membrane. The maximum VOC selectivity of the dual-layer membrane was about 4.6 times that of the PTFE membrane. It is proposed that the increase of organic selectivity is related to the reduced water content in the hydrophilic polyurethane layer, in which organic adsorption decreased the hydrophilicity of the pores. VOC selectivity of the dual-layer membrane declined as the vacuum degree and/or temperature increased due to linear/exponential increase of water flux and almost constant organic flux. The dual layer hydrophilic-hydrophobic membrane swelled slightly when in contact with the synthetic organic solution during the membrane distillation (MD) process but show good resistance to wetting, which is an important feature for practical application of the

membrane for treatment of wastewater containing volatile organic compounds.

Key words: vacuum membrane distillation; volatile organic carbon; wastewater treatment; hydrophilic-hydrophobic membrane

1. Introduction

Volatile organic compounds (VOCs) are organic chemicals that have a high vapour pressure at ordinary room temperature, and exist in solvent thinners, degreasers, cleaners, lubricants, and liquid fuels. These compounds can cause an increase in chemical oxygen demand (COD) of industrial wastewaters [1]. However, perhaps the greatest concern for VOCs emissions is the transport of VOCs from wastewater to air [1]. In the U.S. Title III of the 1990 Clean Air Act Amendments (CAAA), government owned treatment facilities were required to make an inventory of their hazardous air pollutant (HAPs) emissions. Most of the HAPs were identified as VOCs, and regulated by US EPA in discharge to surface water [2, 3].

Membrane distillation (MD) is a membrane-based separation processes using a hydrophobic membrane to isolate the feed and permeate. Depending on the operation mode to decrease the vapor pressure on the permeate side of the membrane [4, 5], MD is classified into four major configurations: direct contact membrane distillation (DCMD), air gap membrane distillation (AGMD), sweeping gas membrane distillation (SGMD), and vacuum membrane distillation (VMD). SGMD and VMD are common configurations considered for VOC removal from aqueous solution [6-12]. However, VOCs are good wetting agents for hydrophobic membranes and, therefore, challenge the use of conventional hydrophobic membranes for MD. In addition, membrane wetting is a particularly important challenge for VMD because the pressure difference between the liquid and membrane pore may be about 100 kPa, which challenges the liquid entry pressure of common membranes used for MD. Hence, wetting abatement is

necessary for successful application of VMD in the removal of VOC from aqueous solutions. Another practical challenge in the use of VMD for VOC removal, is that VMD can only strip VOCs from aqueous solution based on the relative volatility of the organic compounds which is described by Raoult's law, as shown in Equation (1) [13].

Therefore, employing a porous hydrophobic membrane for VOCs removal by MD will not show a performance better than distillation, and would have a high wetting risk that compromises separation efficiency.

$$\alpha_{i,j} = \frac{y_i / x_i}{y_j / x_j} \qquad (1)$$

where $\alpha_{i,j}$ is the relative volatility, y_i and x_i are the molar ratios of the volatile component in the gas phase and liquid phase, and y_j and x_j are the molar ratios of water in the gas phase and liquid phase.

Dual and/or multi-layer hydrophilic-hydrophobic-hydrophilic membranes were introduced for MD in 1982 [14], and were employed for MD flux enhancement and long-term stable operation in desalination process when the hydrophilic layer was facing the permeate stream [15, 16]. However, as we are concerned with reducing potential wetting effects from VOCs, only the configuration with the hydrophilic layer facing the feed is considered. Theoretically, the hydrophilic layer has affinity for the hydrophilic end of an amphiphilic molecule [17], and will leave the other hydrophobic end exposed to the aqueous solution. This action will theoretically convert the hydrophilic pores into partial hydrophobic pores, which will reduce the chance of water molecules accessing the second hydrophobic layer and increase the organic concentration in the hydrophilic layer.

Although there have been many studies that considered dual-layer membranes for anti-wetting

operation and flux enhancement, as far as the authors' are aware, there is a lack of research on the selectivity of the dual-layer membranes for VOC removal.

In this paper, a commercially available PU coated PTFE dual-layer membrane was selected, which had demonstrated anti-wettability in previous work on surfactant laden wastewater [18]. The aim of this research is to identify the potential of the PU coated PTFE membrane for treatment of VOC containing industrial wastewater streams (million litres per day). A synthetic feed that simulated the VOC composition of a real wastewater was used in experiments with membranes that are commercial available, so that the beneficial outcomes could be technically implemented industrially. For comparison purposes a PTFE membrane was also selected, which had demonstrated high hydrophobicity, high flux [19] and similar structure to the PTFE layer in the dual-layer membrane and to other commercially available PTFE membranes.

2. Experimental

2.1 Membrane characterisation

2.1.1 SEM

Scanning electron microscopy (SEM, Merlin ZIESS GEMINI2, Germany) was used to observe the surface and cross section of both membranes. The membrane sample was coated with Iridium for 1-1.5 min before the SEM imaging.

2.1.2 Pore size measurement

Quantachrome Porometer 3G pore size analyser (USA) was used to measure the bubble point pressure, the maximum and average pore diameter of the M1 membrane and the PTFE support of the M2 membrane, using the liquid expulsion technique with wetting liquid Porefil.

The pore size of the PU coating layer of M2 membrane was measured by nitrogen adsorption

with analysis by the Brunauer–Emmett–Teller (BET) model (Micromeritics TriStar Surface Area and Porosity Analyser, GA, USA). Prior to analysis, the sample was degassed at 60°C for 24 h.

2.1.3 Contact angle

The membrane contact angle was measured using the sessile drop method by contact angle analyser (Kruss DSA25, Germany). A 0.5 µL drop was formed on the flat surface of the membrane using a syringe and the contact angle measured by a camera and image analysis. The contact angle of each type of membrane was measured at least 3 times at different positions, and the average value was reported.

2.1.4 Solution uptake test

The solution uptake of the synthetic feed and deionised water by the PU layer was tested at room temperature (20°C). The dry M2 membrane was weighed before the tests. During the test, the PU layer of M2 membrane faced the feed solution in a dead-end cell (diameter 49 mm) under stirring conditions for ~24 hours to wet the hydrophilic layer of M2 membrane. The wetted membrane was then dabbed with kimwipes lightly to remove excess solution and reweighed. The same piece of membrane was used for the both the deionised water and synthetic feed tests. To avoid the organic contamination, the deionised water test was conducted first and dried overnight at 40°C prior to the synthetic feed test. Two pieces of membrane were tested to ensure reproducibility of results.

2.2 VMD testing and theory

2.2.1 VMD experimental

Two membranes were considered for application in VMD for VOC removal: M1, a

microporous PTFE membrane (GE Osmonics: scrim supported PTFE, nominal pore size of 0.45 µm), and M2, a polyurethane coated PTFE dual layer membrane (Australian Textile Mill, Australia, Polyurathane (PU) coated PTFE membrane with textile support). A schematic diagram of the VMD process is shown in Figure 1. A piston pump (Fluid Metering IND. NY, USA) was used to deliver the feed at a flow rate of 30 mL/min. A Sterlitech® CF042D module (WA, USA) was used to accommodate the membranes with an effective area of 0.0042 m^2. The permeate side of the module was positioned downward to allow the salt passed through the membrane to be collected in cold traps for the purpose of checking for wetting of the membrane. Both membranes M1 and M2 were tested in the VMD apparatus. Feed temperatures higher than 45°C (especially at high vacuum pressure) were prone to cause PTFE membrane wetting based on our experimental observation. Furthermore, high temperature commercial waste heat streams are not readily available practically, but waste heat becomes available at temperatures below 60°C, where energy recovery becomes less efficient. Therefore, two feed temperatures at 35^{o} C and 45°C ±5°C were used in the experiments and controlled by a water bath. At each test temperature, three different pressures (-65, -75 and -95 ±5 kPa) were employed using an oil vacuum pump (JAVAC, Australia) and a pressure control valve on a by-pass line (Figure 1).

Before the synthetic feed test, deionised water was used as the feed to test the baseline flux of each type of membrane under the same conditions. The synthetic feed contained 1 wt% sodium chloride and 2.2 wt% VOCs composed of dimethoxymethane, formaldehyde and methanol at a mass ratio of 10:2:1, based on an industrial wastewater composition. To minimise evaporative losses of VOCs, the feed was circulated in an air tight closed loop with a water seal, and the overall mass loss was only from the vapour transfer across the membrane. The feed was sampled every 1 h through a sampling valve, and the membrane flux was calculated based on the feed loss (weight loss of feed tank) that was logged using a balance and a computer. The

feed inlet and outlet temperatures were logged by a thermocouple data logger (PICO, TC-08, UK), and the pressure on the permeate side was monitored by a manometer (TPI-665, USA). Membrane wetting was checked after each experiment by measuring the conductivity of the permeate in the first cold trap. For each type of membrane, three pieces of membrane were used to check the repeatability of the experiments. Each experiment presented in this paper lasted at least 4 h.

The total VOCs concentration in the feed was determined by measuring total organic carbon (TOC, Shimadzu, TOC V with TNM-1 unit, Japan).

2.2.2 Theoretical analysis of the VMD separation

For an ideal mixture, based on Equation (1) and Raoult's law [13], the flux of each component can be calculated by Equation (3) [20, 21].

$$\alpha_{i,j} = \frac{P_i^0}{P_j^0} \qquad (2)$$

where P^0_i, and P^0_j are the vapour pressures of volatiles and water at temperature T.

$$J_i = -C_m \sqrt{M} \Delta P_i \qquad (3)$$

where J_i is the flux of the component across the membrane, C_m is the mass transfer coefficient that is related to the membrane properties, M is the molecular weight, and ΔP_i is the vapour pressure difference of the component across the membrane that can be calculated using Equation (4) based on Dalton's law [13]:

$$\Delta P = y_i \cdot P_{total} - x_i P_i^0 \qquad (4)$$

where the P_{total} is the total pressure on the permeate side of the membrane.

VOC removal from the feed can be expressed as the depletion ratio as shown in Equation (5).

$$R = \frac{C_0 - C}{C_0} \quad (5)$$

where R is the depletion ratio calculated as the ratio of depleted VOC concentration (C_0 - C) of the treated water to the original VOC concentration (C_0) in the feed, and C is the measured VOC concentration in the feed at a certain recovery.

The feed recovery was calculated by Equation (6).

$$Recovery = \frac{m_0 - m}{m_0} \times 100\% \quad (6)$$

where *Recovery* is the percentage of the water depleted from the feed, m is the mass of treated water, and m_0 is the original feed mass.

The water flux of the membrane was calculated by Equation (7).

$$J = \frac{m_0 - m}{A \cdot t} \quad (7)$$

Here, A is the area of the membrane and t is the time.

Since the organic flux varied with VOC concentration (organic vapour pressure, Equation (3)) at different feed recovery, the normalized organic flux calculated by Equation (8) was used in this study.

$$J_{norm} = \frac{J_{voc}}{C} = \frac{\Delta C}{A \cdot t \cdot C} \quad (8)$$

where J_{norm} is normalised VOC flux, J_{voc} is the VOC flux at certain feed recovery, and ΔC is the VOC change during time t.

Because the water is the main component (> 96 wt%), the flux change with time due to its

molar ratio variation can be ignored. Therefore, the selectivity of the VOC by the membrane is here defined as,

$$Se = \frac{J_{norm}}{J} \tag{9}$$

where *Se* is the membrane selectivity to VOC.

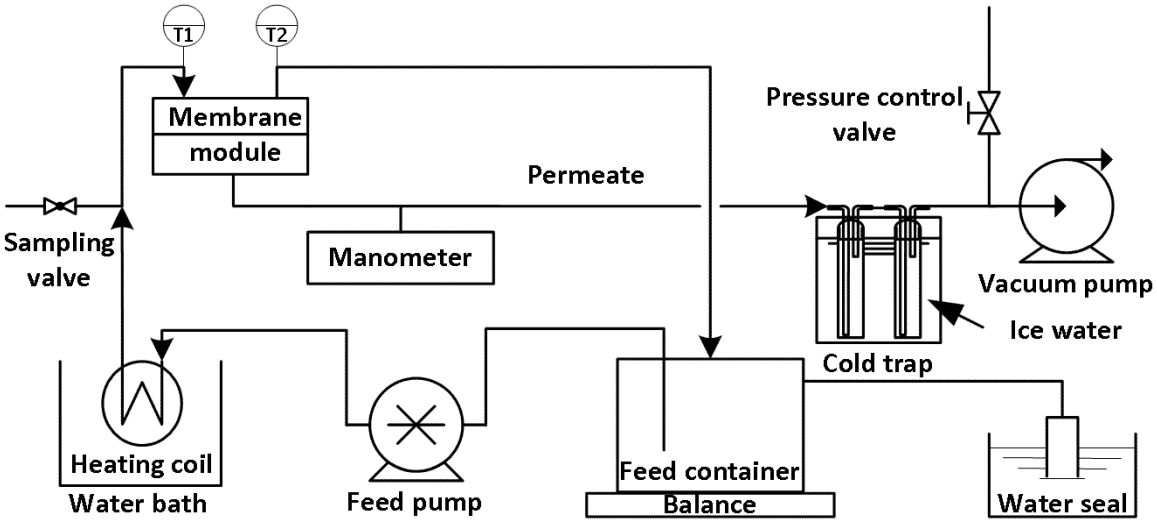

Figure 1. Schematic of the VMD process

3. Results and discussion

3.1 Membrane characterisation

Table 1 lists the contact angles of both membranes with deionised water and synthetic feed. It can be seen that the contact angles of both membranes declined due to the reduced surface tension of the feed solution by the added organics. However, the influence of the feed showed greater influence on the contact angle of the dual layer membrane than that of the PTFE membrane, due to the higher organic affinity of PU than that of PTFE.

Table 1. Contact angles of feed solution and deionised water on M1 and M2 membranes

Membrane type	Contact angle (°)	
	Water	Synthetic Feed
M1	139±2	134±2
M2	59±2	51±2

SEM images for both membranes are shown in Figure 2. The surface of the PTFE membrane (M1) was porous and had a network structure composed of knots and fibrils (Fig. 2-a1), but the PU layer of the dual-layer membrane (M2) was dense and rough with many protruding lumps (Fig. 2-b1). The cross section images of both membranes are shown in Figures 2.-a2 and 2.-b2. It was noted that delamination of the dual layer membrane occurred during sample preparation. M1 has a PTFE thickness of approximately 70 µm, which is about 2.4 times of the overall dual layer thickness (29 µm, PU layer + PTFE layer) of the M2 membrane (excluding the textile support), and about 4 times the thickness of the M2 PTFE layer (18 µm) sandwiched between the PU coating layer and the textile support layer. Therefore, the vapour mass transfer resistance due to the PTFE membrane thickness of the M2 membrane was only 1/4 that of the M1 membrane [22] (resistance proportional to thickness), assuming that only liquid water passed through the PU layer.

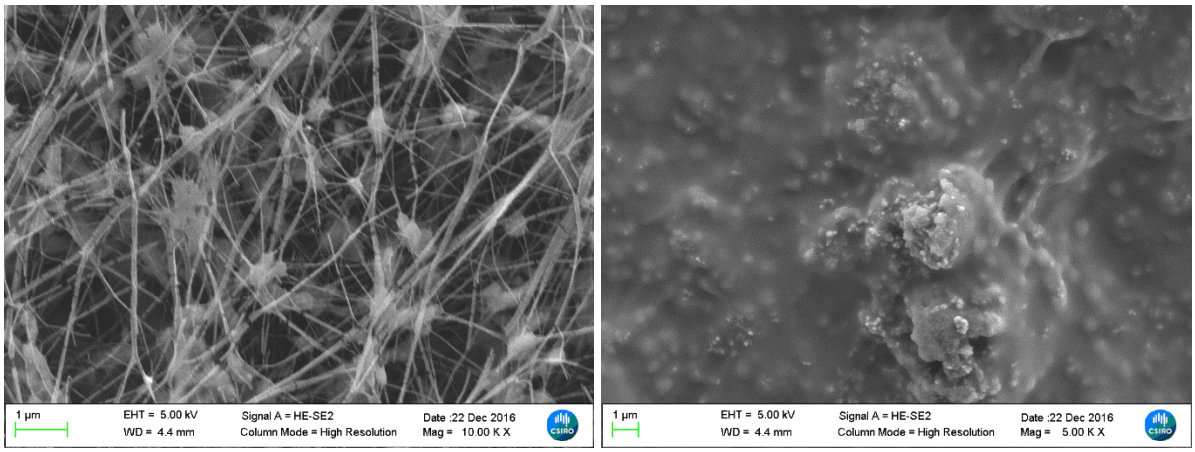

a1. M1 surface b1. M2 Surface

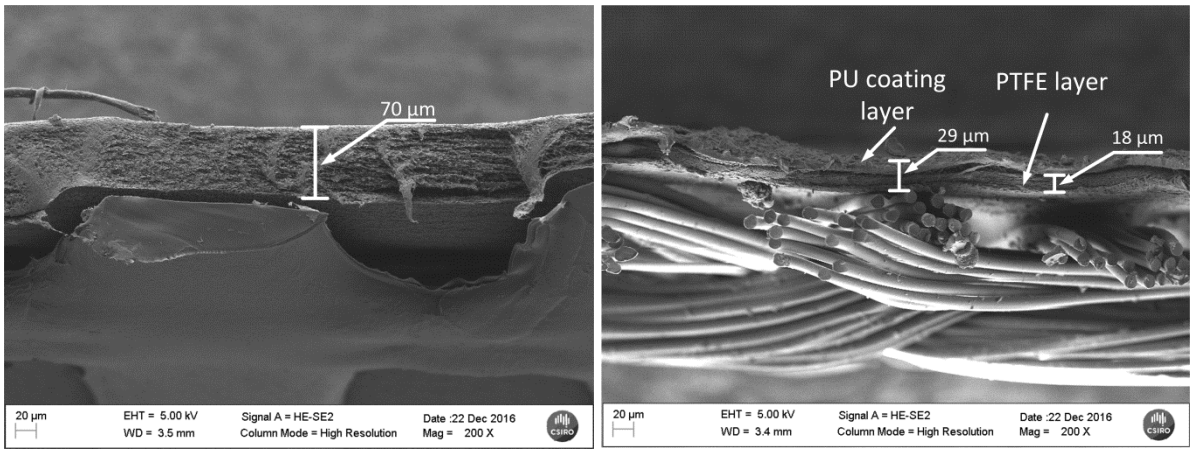

a2. M1 cross section b2. M2 cross section

Figure 2. Surface and cross section morphology of PTEF membrane (M1) and dual-layer hydrophilic and hydrophobic membrane (M2)

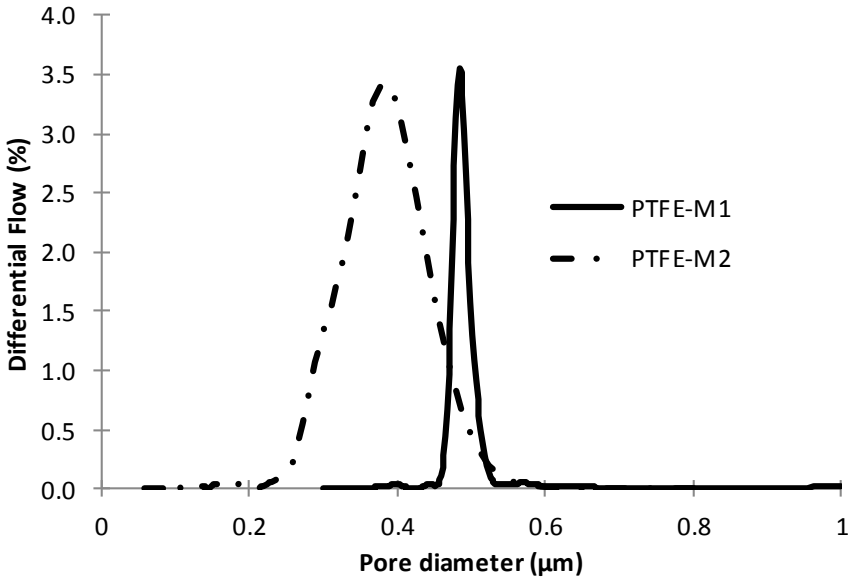

a. Pore size distribution of M1 membrane and the PTFE layer of M2 membrane

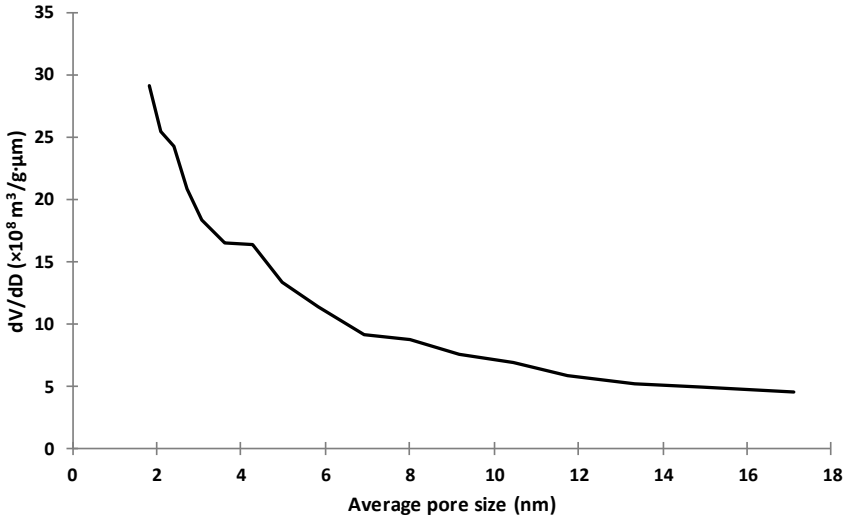

b. Pore size distribution of M2 PU coating layer

Figure 3. M1 and M2 membrane pore size measurement

Figure 3a shows the pore size distributions of the M1 membrane and PTFE layer of M2 membrane. It can be seen that the PTFE layer of the M2 membrane had relatively smaller mean pore size (Table 2), but wider pore size distribution than that of the M1 membrane. Assuming the flux has a square relationship to the membrane pore size [23], the vapour mass transfer resistance due to membrane pore size of M2 is about 1.8 times that of M1. Therefore, the estimated ratio of the mass transfer resistance of M1 to M2 PTFE layer based on Equation (10) [19] and the relative pore size and thickness measurements was about 2.2 times, assuming the PTFE layers had similar porosity and tortuosity [24-26].

$$\frac{R_{M1}}{R_{PTFE}} = \frac{b_{M1}\cdot\tau_{M1}}{r_{M1}^{\ 2}\varepsilon_{M1}} \div \frac{b_{M2}\cdot\tau_{M2}}{r_{M2}^{\ 2}\varepsilon_{M2}} = \frac{b_{M1}\cdot r_{M2}^{\ 2}}{b_{M2}\cdot r_{M1}^{\ 2}} = \frac{70\times 0.36^2}{18\times 0.48^2} \approx 2.2 \qquad (10)$$

where the R_{M1} and R_{PTFE} are the mass transfer resistance of PTFE layer of the M1 and M2 membrane, b_{M1} and b_{M2} are the PTFE layer thicknesses of the M1 and M2 membranes, r_{M1} *and* r_{M2} are the mean PTFE layer pore radiuses of the M1 and M2 membranes, ε_{M1} and ε_{M2} are the PTFE layer porosity of the M1 and M2 membranes, and τ_{M1} and τ_{M2} are the PTFE layer pore

tortuosity of the M1 and M2 membranes.

Table 2. Pore size and bubble point of M1 membrane and PTFE layer of M2 membrane

Membrane	Maximum Pore Size (μm)	Mean Flow Pore Size (μm)	Minimum Pore Size (μm)	Bubble Point Pressure (bar)
M1	0.57	0.48	0.30	1.12
M2 - PTFE	0.45	0.36	0.11	1.41

Due to its smaller size being below the detection limit of the Porometer employed, the pore size distribution of the PU layer of M2 membrane was measured by BET. As shown in Figure 3b, the pore size of the PU layer was largely less than 10 nm and the peak appeared at approximately 2 nm, where the BET measurements were unable to detect pores less than this.

The solution uptake results are listed in Table 3. It can be seen that the PU layer absorbed less feed than deionised water. This test demonstrated that the existing amphiphilic organic molecule has partially converted the pores from hydrophilic to hydrophobic, which reduced the water content in the PU layer.

Table 3 Solution uptake test for the PU layer

Test	Test1 (g/m^2)	Test2 (g/m^2)	Average (g/m^2)
Deionised water	26.1	21.5	23.8
Synthetic feed	18.5	17.4	18.0

3.2 VMD testing

3.2.1 Comparison of deionised water flux

In Figure 4, the deionised water flux of membranes M1 and M2 under different vacuum pressures and temperatures are shown. When the feed temperature or vacuum pressure increased, water flux for both membranes increased exponentially, and the M1 flux increased much faster than that of M2. The M1 flux was about the same as the M2 flux at 35°C under vacuum pressure of 65 and 75 kPa (Figure 4a), but was about twice that of the M2 flux at 45°C under the same vacuum pressures (Figure 4b). When the vacuum pressure increased to 95 kPa, the M1 flux increased to more than double of the M2 flux at 35°C and almost triple that of the M2 flux at 45°C. Since the theoretical flux of the M2 PTFE membrane should be 2.2 times of that of the M1 PTFE membrane based on the mass transfer resistance across the PTFE layers under the same conditions, the lower flux of M2 membrane should be due to the resistance from the PU coating layer. Since it is assumed that only liquid phase passes through the PU layer, the mass transfer across the membrane can be considered similar to filtration, where the flux is linear to the driving force [27]. Under stable conditions, the mass transfer across the PU layer should equal to the mass transfer across the PTFE layer as shown in Equation (11).

$$J_{M2} = \frac{\Delta P_{PU}}{R_{PU}} = \frac{\Delta P_{PTFE}}{R_{PTFE}} = \frac{P_{feed} - P_{permeate,PU}}{R_{PU}} = \frac{P_{vap,PU} - P_{vap,PTFE}}{R_{PTFE}} = \frac{(P_{feed} - P_{vap,PTFE}) + (P_{vap,PU} - P_{permeate,PU})}{R_{PU} + R_{PTFE}} \quad (11)$$

Here, ΔP_{PU} is the hydraulic pressure difference across the PU layer, R_{PU} is the mass transfer resistance of the PU layer, ΔP_{PTFE} is the vapour pressure difference across the PTFE layer, P_{feed} is the absolute hydraulic pressure of the feed, $P_{permeate,PU}$ is the absolute total pressure on the permeate side of the PU layer, the $P_{vap,PU}$ is the vapour pressure on the permeate side of the PU layer, $P_{vap,PTFE}$ is the vapour pressure on the permeate side of the PTFE layer, and the R_{PTFE} is the mass transfer resistance of PTFE layer. Since the gas phase on PU layer permeate side was

at low pressure, it could be considered an ideal gas mixture and the air partial pressure (stagnant gas) was the same across the pore. Therefore,

$P_{permeate,PU} = P_{air} + P_{vap,PU}$, and

$$P_{vap,PTFE} = y_{vap,PTFE} P_{total,PTFE} = y_{vap,PTFE}(P_{atm} - P_{vacuum})$$

Equation (11) can be expressed as Equation (12).

$$J_{M2} = \frac{(P_{feed} - (P_{atm} - P_{vacuum}) y_{vap,PTFE}) - P_{air}}{R_{PU} + R_{PTFE}} = \frac{(P_{feed} - (P_{atm} - P_{vacuum}) y_{vap,PTFE}) - P_{air}}{R_{PU} + R_{PTFE}} \quad (12)$$

The feed gauge pressure was only about 1-2 kPa, thus, P_{feed} approximately equals P_{atm}.

Due to:

$P_{vacuum} = P_{atm} - P_{air}$, Equation (12) can be rewritten as

$$J_{M2} \approx \frac{P_{vacuum} - (P_{atm} - P_{vacuum}) y_{vap,PTFE}}{R_{PU} + R_{PTFE}} \quad (13)$$

where $y_{vap,PTFE}$ is the vapour molar ratio on PTFE layer permeate side, P_{air} is the absolute air pressure in the PTFE layer of M2 membrane, and P_{atm} and P_{vaccum} are the atmospheric and vacuum pressures respectively.

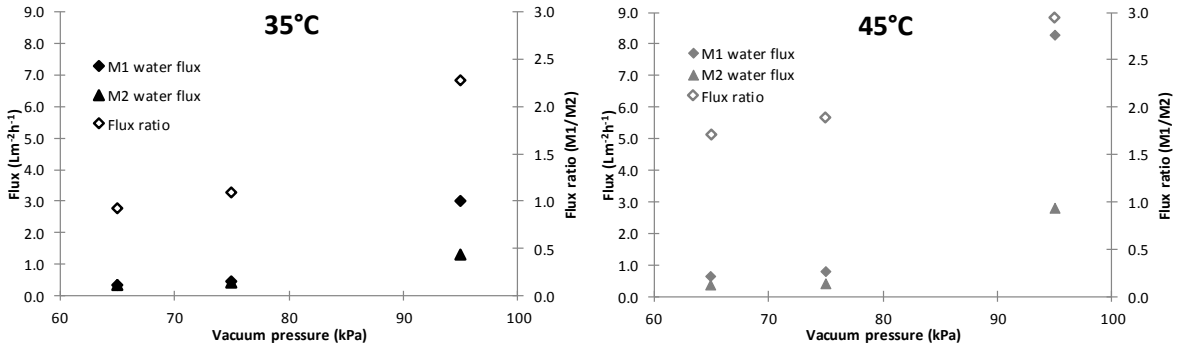

a. b.

Figure 4. Deionised water flux of M1 and M2 under different vacuum pressures and temperatures (flowrate = 30 mL/min, error = ± 5)

The mass transfer across the M1 membrane can be expressed as Equation (14).

$$J_{M1} = \frac{\Delta P}{R_{M1}} = \frac{P_{vap,feed} - P_{vap,permeate}}{R_{M1}} = \frac{P_{vap,feed} - (P_{atm} - P_{vacuum}) y_{permeate}}{R_{M1}} \quad (14)$$

where J_{M1} is the M1 flux, ΔP is the vapour pressure difference across the membrane, R_{M1} is the mass transfer resistance across M1 membrane, $P_{vap,feed}$ is the vapour pressure on the M1 feed side, $y_{permeate}$ is the vapour molar ratio on M1 permeate side, and $P_{vap,permeate}$ is the vapour pressure on the M1 permeate side.

Since the two membranes showed similar flux at 35°C and 65 kPa (Figure 4a) and the gas pumping flowrate of the vacuum pump is only related to the vacuum pressure, it can be concluded that the vapour partial pressures on the permeate side of the M1 and M2 membranes should be similar at this operating condition. Therefore,

$$(P_{atm} - P_{vacuum}) y_{permeate} \approx (P_{atm} - P_{vacuum}) y_{vap,PTFE} \quad (15)$$

In a system under stable vacuum pressure, the air can be considered as a stagnant component. Therefore, the air pressure in the system should be the same and no greater than the absolute pressure in the system. Thus, under 65 kPa vacuum pressure, the air pressure in the system should be less than 36 kPa (assuming atmospheric pressure is 101 kPa). The feed vapour pressure should be less than vapour pressure at 35°C due to temperature polarisation, which is only 5.6 kPa [28] in Equation (14). Since J_{M1} is a positive value, $(P_{atm} - P_{vacuum})y_{permeate}$ should be less than 5.6 kPa. Therefore, based on Equation (15), $(P_{atm} - P_{vacuum})y_{vap,PTFE}$ should be less than 5.6 kPa, and the numerator in Equation (13), $P_{vacuum} - (P_{atm} - P_{vacuum})y_{vap,PTFE}$, should be greater than (65 -5.6) = 59.4 kPa. Since $J_{M1} \approx J_{M2}$ and the numerator in Equation (14) is less than 5.6 kPa, the denominator in Equation (13) should be greater than 10.6 times denominator in Equation (14). Therefore, it can be concluded that the mass transfer resistance ($R_{PU} + R_{PTFE}$) of the M2 membrane is at least about 10.6 times of R_{M1} of the M1 membrane. However, because

the R_{M1} is 2.2 times of R_{PTFE} , the major mass transfer resistance is from the PU coating layer.

Based on Equations (13) and (14), it can be found that as the vacuum pressure (P_{vacuum}) increased the flux of both membranes increased. The enlarged flux difference in Figures 4a and 4b at high vacuum pressure between M1 and M2 membranes is due to their mass transfer resistance difference. The mass transfer resistance of the M2 membrane is at least 10.6 times that of the M1 membrane, and the mass transfer coefficient is defined as the inverse of the mass transfer resistance as shown in Equations (3) and (11). In Figure 1S, the flux of the M2 membrane is normalised against that of the M1 membrane based on Equation (3) under the same driving force. It can be seen that as the driving force increases, the flux difference between the M1 and M2 membrane becomes greater.

3.2.2 Organic removal tests

In Figure 5, the VOC depletion ratio for different membranes is shown. It can be seen that the maximum VOC removals of M1 and M2 membrane achieved were about 90% (50% water recovery at 45^{o} C and 95 kPa) and 72% (30% water recovery at 45^{o} C and 75 kPa), respectively.

In Figure 5a, it also can be seen that the VOC removal of M1 membrane showed a strong relationship to the recovery, but a weak relationship to the temperatures and vacuum pressures. As shown in Table 4, the molar ratio of the organics in the feed solution was about 0.7%. Therefore, the solution was very dilute and could be considered as an ideal solution. The partial vapour pressure and relative volatility calculated based on an ideal solution is shown in Table 4 [29]. For a distillation process, the separation of different components depends on the volatility difference (vapour pressure difference) as shown in Equation (2). For ideal solutions, the reduced ambient pressure (increased vacuum pressure) will accelerate the mass transfer rates of all components based on Equations (3) and (4), but will not alter the volatility

difference [29]. Therefore, the composition in the vapour phase will be determined by the composition in the liquid phase at the same temperature, which was also demonstrated in Figure 5a as the VOC depletion ratio only changed with feed recovery at the same temperature. In Table 4, the vapour pressures of the components in the feed solution at different temperatures are listed. As the temperature increased from 35°C to 45°C, it can be seen that the water vapour pressure had the greatest increase. Therefore, based on Equations (1) and (2), the relative volatility between the VOCs and the water became smaller with increasing temperature. It also can be seen from Figure 5a that the organic depletion ratio at 35°C was higher than that at 45°C for recoveries lower than 20%. However, the depletion ratio difference between different temperatures reduced, because the higher VOC flux resulted in a lower VOC concentration in the feed and supressed the VOC mass transfer rate.

Table 4. Molar ratio and partial vapour pressure of all components

Component	Molar ratio	Partial vapour pressure (kPa)		Relative volatility to Water		Vapour pressure increment (%)
		35°C	45°C	35°C	45°C	
Water	0.993	5.6	9.6	1	1	71%
Formaldehyde	0.004	1.32	1.74	58	45	32%
Methanol	0.002	0.29	0.46	25	24	59%
Dimethoxymethane	0.001	0.32	0.46	56	48	44%

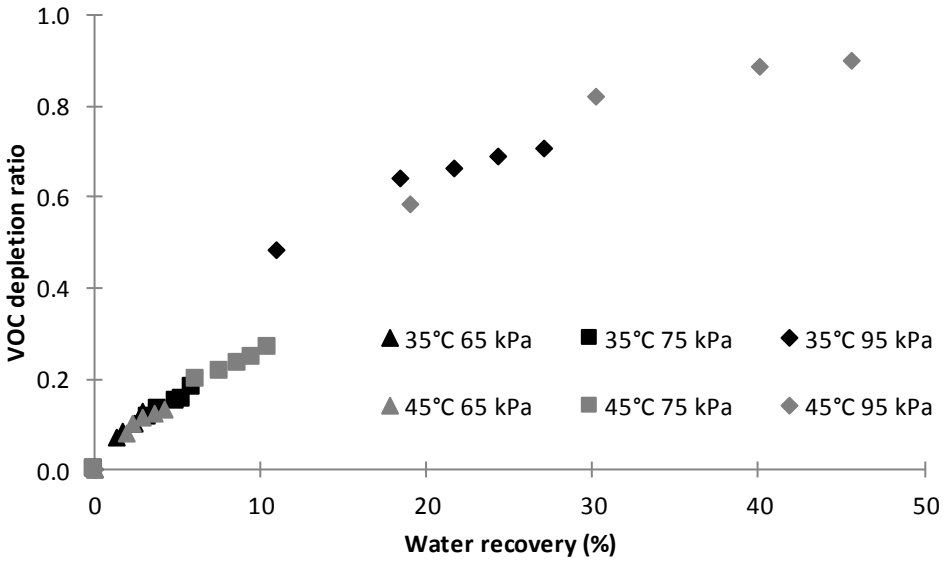

a. M1 membrane

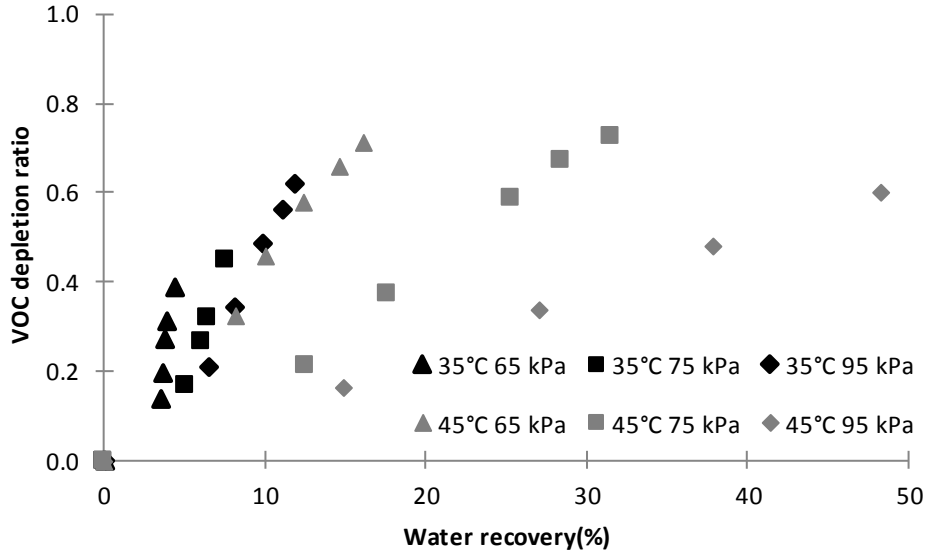

b. M2 membrane

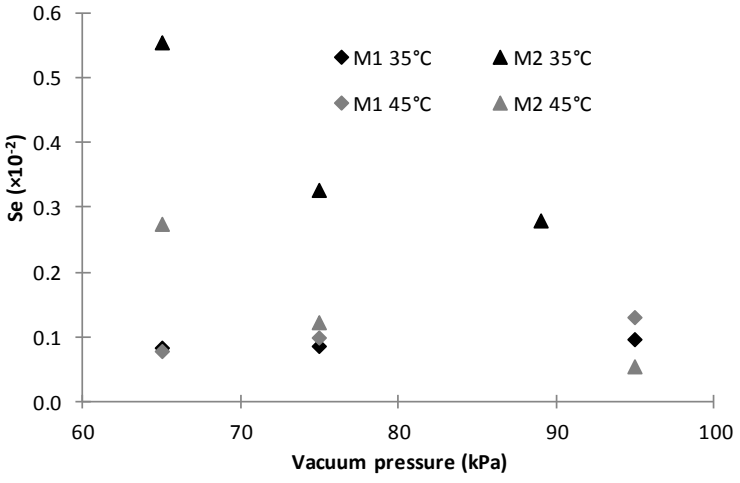

c. VOC selectivity of M2 and M1

Figure 5. Organic depletion ratio and selectivity at different feed recoveries for various vacuum pressures (flowrate = 30 mL/min, error = ±5%)

In Figure 5b, the VOC depletion ratio using M2 membrane is shown. It can be seen that the VOC depletion ratio varied with both the temperature and vacuum pressure. The depletion ratio at high vacuum pressure and temperature is less than that at low vacuum pressure and temperature at the same recovery. A depletion ratio of 0.4 was achieved with 4.4% feed recovery at 65 kPa and 35°C.

It also can be seen from Figure 5c that the PTFE (M1) membrane selectivity only change slightly with vacuum pressure and temperature. However, the VOC selectivity of the M2 membrane decreased dramatically with increasing vacuum pressure and temperature. The dramatic decline of the VOC selectivity can be attributed to the difference of the dominant mass transfer resistance between water and the VOC at different temperature and vacuum degree. From Figures 7a and 7b, it can be found that as the vacuum pressure increased from 65 to 95 kPa, the M2 water flux increased by 3 and 5 times respectively at 35°C and 45°C, but the normalized VOC flux of M2 membrane remained almost unchanged at 45°C and increased by approximately 50% at 35°C. The water flux of M2 membrane is determined by the hydraulic pressure difference across the hydrophilic layer of the M2 membrane. As the vacuum pressure increased, it can be found from Equation (11) that the water flux will increase. However, the selectivity of the organics and/or the rejection of water molecules (demonstrated by the water uptake test) depends on the hydrophobicity, which will not alter under different vacuum pressures. The rate of the overall organics carried by the feed (high flux) transferred across the hydrophilic layer will become greater under higher vacuum degree due to the higher hydraulic pressure across the PU layer (ΔP_{PU}) as shown in

Equation (11). The organic concentrated in the PU layer would be diluted more by the feed with lower organic concentration at higher flux. Therefore, it can be seen at 35°C that the VOC flux of M2 membrane increased (Figure 6b) due to the increased VOC transfer rate with increasing vacuum pressure, but VOC selectivity decreased (Figure 5b) due to the reduced organic concentration in the hydrophilic layer.

In comparison to the M1 VOC selectivity in Figure 5c, it can be found that the M2 membrane showed better VOC selectivity under most test conditions, except for under 95 kPa at 45°C. The maximum organic selectivity of M2 membrane was about 4.6 times that of the M1 membrane. Since the organic selectivity of the M1 membrane is based on distillation separation following Raoult's law, the higher organic selectivity of the M2 membrane demonstrated that organic removal by the M2 membrane did not follow Raoult's law. It is proposed that the high VOC selectivity of M2 membrane is due to the ability of PU to absorb VOC [30]. Furthermore, the affinity of the hydrophilic layer to the hydrophilic end of an amphiphilic molecule [17] will leave the other hydrophobic end exposed to the aqueous solution and theoretically convert the hydrophilic pores into partial hydrophobic pores, which has been demonstrated by the water uptake tests. This behaviour will reduce the chance of water molecules accessing the second hydrophobic layer (reducing wetting risk) and increase the organic concentration in the hydrophilic layer, which also facilitates VOC selectivity of the M2 membrane.

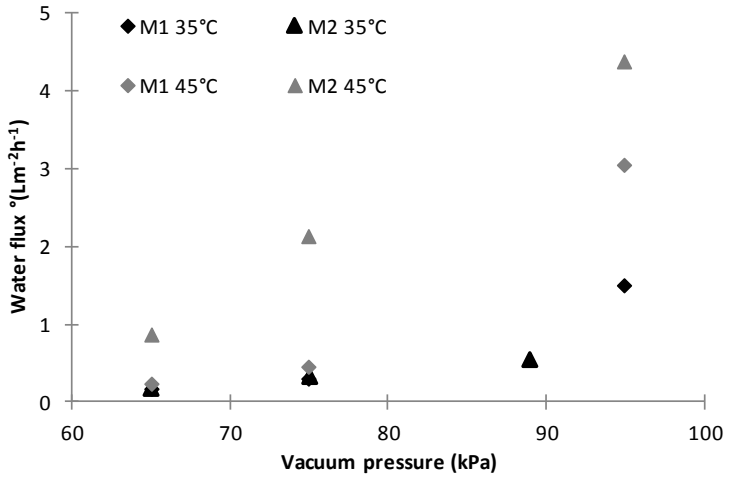

a. Water flux at different temperatures and vacuum pressures

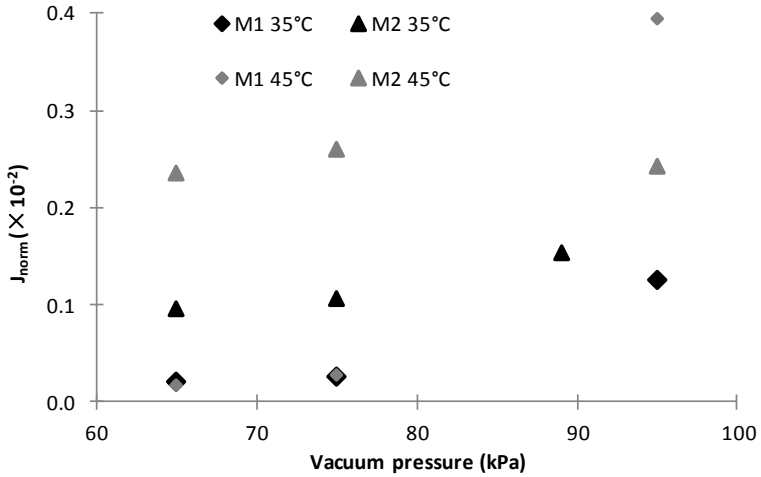

b. Normalized VOC flux at different temperatures and vacuum pressures

Figure 6. Mean water flux and relative VOC flux (flowrate = 30 mL/min, error = ±5%)

In comparison with the water flux of the M1 membrane in Figure 6a, it can be seen that the water flux increment of the M2 membrane increased as the temperature rose from 35 to 45°C under the same vacuum pressure. However, in Figure 4, the deionised water flux of the M1 membrane was higher than that of M2 membrane under the same conditions. The operating parameters of the VOC removal tests were maintained the same as the deionised water tests, except for the VOC in the feed. Therefore, it is proposed that the interactions between the PU

layer and VOCs altered the mass transfer characteristics of the PU layer at 45°C, which also led to the almost unchanged VOC flux in Figure 6b. Previous studies have demonstrated the swelling of the PU polymer caused by organic compounds/solvents such as ethanol and chlorobenzene [31, 32] that can lead to a change of the membrane porosity and pore size [33]. Based on the experimental results in this study, the presence of VOC led to the swelling of the PU layer of M2 based on the increased water permeability, especially at elevated temperature.

A dramatic increase of the normalised VOC flux of the M1 membrane under the vacuum pressure of 95 kPa in Figure 6b, which is due to the feed solution vapour pressure based on [34] being greater than the reduced absolute vacuum pressure (i.e. VOCs boil at that vacuum pressure).

Therefore, the low vacuum pressure and low temperature will facilitate the selectivity of the M2 membrane as shown in Figure 5c, which will also reduce the water vapour transfers through the membrane and reduce the vacuum energy consumption (Figure 4). As shown in Figure 6, although the low vacuum pressure would not have significant impact on the organic flux, the organic flux reduced 30 - 60% when reducing the feed temperature from 45°C to 35°C. Thus, there is trade-off between the selectivity and organic flux, depending the requirement of the wastewater treatment.

3.2.3 Wetting resistance

Although for all the results presented the salt rejections were higher than 99%, membrane wetting occurred for the M1 membrane after it was left in the module with feed for an extended period (>2 days). For the M2 membrane, there was no wetting issue for similar feedwater exposure times, possibly due to the partial conversion of pore from hydrophilic to hydrophobic. However, further study is needed to verify the mechanism of wetting prevention.

3.3 Research in the future

Although M2 membrane showed reasonable removal and anti-wetting performance for treating VOCs in VMD, the membrane is far from optimal. The PU layer seemed to swell in the organic solution and both high temperature and vacuum pressure could cause the deterioration of the VOC selectivity. Therefore, a membrane with organic stable hydrophilic layer is necessary for removal organic at high temperature.

4. Conclusion

The mechanism of a dual-layer hydrophilic-hydrophobic membrane for selective organic removal was discussed and compared to the performance of a porous PTFE membrane.

The dual layer membrane showed increased VOC selectivity due to the PU coating layer absorbing VOCs and the high affinity of the PU layer to the organic hydrophilic end, which reduced the water content and increased the organic concentration in the hydrophilic layer. The maximum VOC selectivity of the dual-layer membrane was about 4.6 times of that of the PTFE membrane.

Although the membrane structure was not optimised, the dual layer membrane showed relatively high selectivity of VOC at low temperature and vacuum pressure. 0.4 organic depletion ratio (40% organic removed) was achieved with 4.4% water recovery at 35°C with vacuum pressure of 65 kPa. The selectivity difference of the dual layer membrane under different temperatures and vacuum pressures was due to the mass transfer competition across the hydrophilic layer. High temperature and vacuum pressure will encourage both the water and VOC flux, but the magnitude of water flux increase was greater than that of the VOC flux. The VOC selectivity of the dual layer membrane was less than that of the single layer PTFE membrane at 45°C and 95 kPa, and it is proposed that this was due to the membrane swelling.

The dual layer membrane showed better wetting resistance than the single layer PTFE membrane.

Therefore, developing a membrane with stable hydrophilic-hydrophobic layer can be promising for VOC removal.

Nomenclature

$\alpha_{i,j}$	relative volatility
A	membrane area
b	Membrane thickness
C	VOC concentration in the feed
ΔC	VOC change during time t
C_m	membrane mass transfer coefficient
ε	membrane porosity
J_i	flux of the component across the membrane
J_{M1}	flux of M1 membrane
J_{norm}	normalised VOC flux
J_{voc}	VOC flux at certain feed recovery
m	mass of treated water
m_0	original feed mass
M	molecular weight
P_{air}	absolute air pressure in the PTFE layer of M2 membrane
P_{atm}, P_{vaccum}	atmospheric and vacuum pressures respectively
P_{feed}	absolute hydraulic pressure of the feed,
P_{total}	total pressure on the permeate side of the membrane
$P_{permeate,PU}$	absolute total pressure onthe permeate side of the PU layer
$P_{vap,feed}$	vapour pressure on the M1 feed side

$P_{vap,permeate}$	vapour pressure on the M1 permeate side
$P_{vap,PTFE}$	vapour pressure on the permeate side of the PTFE layer
$P_{vap,PU}$	vapour pressure on the permeate side of the PU layer
P^0_i, P^0_j	vapour pressures of volatiles and water at temperature T
ΔP	vapour pressure difference across the membrane
ΔP_i	vapour pressure difference of the component across the membrane
ΔP_{PU}	hydraulic pressure difference across the PU layer
ΔP_{PTFE}	vapour pressure difference across the PTFE layer
R_{PTFE}	mass transfer resistance of PTFE layer of M2 membrane
r	mean membrane pore radius
R	depletion ratio
Recovery	percentage of the water depleted from the feed
R_{M1}	mass transfer resistance across M1 membrane
R_{PU}	mass transfer resistance of the PU layer
Se	membrane selectivity to VOC
t	time
τ	the membrane pore tortuosity
x_i	molar ratios of the volatile component in liquid phase
y_i	molar ratios of volatile component in gas phase
$y_{permeate}$	vapour molar ratio on M1 permeate side
$y_{vap,PTFE}$	vapour molar ratio on PTFE layer permeate side

Reference

[1] P. Hunter, S.T. Oyama, Control of volatile organic compound emissions, John Wiley, 2000.
[2] W.-H. Cheng, S.-K. Hsu, M.-S. Chou, Volatile organic compound emissions from wastewater treatment plants in Taiwan: Legal regulations and costs of control, Journal of Environmental Management, 88 (2008) 1485-1494.
[3] Organic Chemicals, Plastics and Synthetic Fibers Effluent Guidelines, in: USEPA (Ed.), 1987.
[4] A.M. Alklaibi, N. Lior, Membrane-distillation desalination: Status and potential, Desalination, 171 (2005) 111-131.
[5] K. Smolders, A.C.M. Franken, Terminology for Membrane Distillation, Desalination, 72 (1989) 249-262.
[6] C.A. Rivier, M.C. García-Payo, I.W. Marison, U. von Stockar, Separation of binary mixtures by thermostatic sweeping gas membrane distillation: I. Theory and

simulations, Journal of Membrane Science, 201 (2002) 1-16.
[7] L. Basini, G. D'Angelo, M. Gobbi, G.C. Sarti, C. Gostoli, A desalination process through sweeping gas membrane distillation, Desalination, 64 (1987) 245-257.
[8] M. Khayet, P. Godino, J.I. Mengual, Theory and experiments on sweeping gas membrane distillation, Journal of Membrane Science, 165 (2000) 261-272.
[9] M. Khayet, P. Godino, J.I. Mengual, Nature of flow on sweeping gas membrane distillation, Journal of Membrane Science, 170 (2000) 243-255.
[10] M.C. Garcia-Payo, C.A. Rivier, I.W. Marison, U. von Stockar, Separation of binary mixtures by thermostatic sweeping gas membrane distillation: II. Experimental results with aqueous formic acid solutions, Journal of Membrane Science, 198 (2002) 197-210.
[11] S. Bandini, C. Gostoli, G.C. Sarti, Separation efficiency in vacuum membrane distillation, Journal of Membrane Science, 73 (1992) 217-229.
[12] G.C. Sarti, C. Gostoli, S. Bandini, Extraction of organic components from aqueous streams by vacuum membrane distillation, Journal of Membrane Science, 80 (1993) 21-33.
[13] I.J. Halvorsen, S. Skogestad, Distillation theory, Encyclopedia of Separation Science, (2000) 1117-1134.
[14] D.Y. Cheng, S.J. Wiersma, Composite membrane for a membrane distillation system, in, US, 1982.
[15] S. Bonyadi, T.S. Chung, Flux enhancement in membrane distillation by fabrication of dual layer hydrophilic–hydrophobic hollow fiber membranes, Journal of Membrane Science, 306 (2007) 134-146.
[16] F. Edwie, M.M. Teoh, T.-S. Chung, Effects of additives on dual-layer hydrophobic–hydrophilic PVDF hollow fiber membranes for membrane distillation and continuous performance, Chemical Engineering Science, 68 (2012) 567-578.
[17] A.D. McNaught, A. Wilkinson, Compendium of Chemical Terminology, in, International Union of Pure and Applied Chemistry, 1997, pp. 1670.
[18] D. Cheng, J. Zhang, N. Li, D. Ng, S.R. Gray, Z. Xie, Antiwettability and Performance Stability of a Composite Hydrophobic/Hydrophilic Dual-Layer Membrane in Wastewater Treatment by Membrane Distillation, Industrial & Engineering Chemistry Research, 57 (2018) 9313-9322.
[19] J. Zhang, N. Dow, M. Duke, E. Ostarcevic, J.-D. Li, S. Gray, Identification of material and physical features of membrane distillation membranes for high performance desalination, Journal of Membrane Science, 349 (2010) 295-303.
[20] M.A. Izquierdo-Gil, G. Jonsson, Factors affecting flux and ethanol separation performance in vacuum membrane distillation (VMD), Journal of Membrane Science, 214 (2003) 113-130.
[21] S. Bandini, C. Gostoli, G. Sarti, Separation efficiency in vacuum membrane distillation, Journal of Membrane Science, 73 (1992) 217-229.
[22] J. Zhang, S. Gray, J.-D. Li, Modelling heat and mass transfers in DCMD using compressible membranes, Journal of Membrane Science, 387–388 (2012) 7-16.
[23] J. Zhang, J.-D. Li, M. Duke, M. Hoang, Z. Xie, A. Groth, C. Tun, S. Gray, Modelling of vacuum membrane distillation, Journal of Membrane Science, 434 (2013) 1-9.
[24] J. Zhang, N. Dow, M. Duke, E. Ostarcevic, S. Gray, Identification of material and physical features of membrane distillation membranes for high performance desalination, Journal of Membrane Science, 349 (2010) 295-303.
[25] J. Zhang, J.-D. Li, S. Gray, Effect of applied pressure on performance of PTFE membrane in DCMD, Journal of Membrane Science, 369 (2011) 514-525.
[26] J. Zhang, Theoretical and experimental investigation of membrane distillation, in,

Victoria University, 2011.
[27] J. Ní Mhurchú, G. Foley, Dead-end filtration of yeast suspensions: Correlating specific resistance and flux data using artificial neural networks, Journal of Membrane Science, 281 (2006) 325-333.
[28] R.E. Sonntag, C. Borgnakke, G.J. Van Wylen, S. Van Wyk, Fundamentals of thermodynamics, Wiley New York, 1998.
[29] J. Smith, H. Van Ness, M. Abbott, Chemical engineering thermodynamics, Sat, 18 (1996) 1-3.
[30] E. Scholten, L. Bromberg, G.C. Rutledge, T.A. Hatton, Electrospun polyurethane fibers for absorption of volatile organic compounds from air, ACS applied materials & interfaces, 3 (2011) 3902-3909.
[31] J.H. Lee, S.C. Kim, Hydrophilic-hydrophobic interpenetrating polymer networks (IPN's) synthesized under high pressure. 1. Morphology, dynamic mechanical properties, and swelling behavior of polyurethane-polystyrene IPN's, Macromolecules, 19 (1986) 644-648.
[32] S. Ajithkumar, N. Patel, S. Kansara, Sorption and diffusion of organic solvents through interpenetrating polymer networks (IPNs) based on polyurethane and unsaturated polyester, European polymer journal, 36 (2000) 2387-2393.
[33] A. Sharma, S.P. Thampi, S.V. Suggala, P.K. Bhattacharya, Pervaporation from a Dense Membrane: Roles of Permeant− Membrane Interactions, Kelvin Effect, and Membrane Swelling, Langmuir, 20 (2004) 4708-4714.
[34] Y.A. Cengel, M.A. Boles, Thermodynamics: an engineering approach, 6th ed., McGraw-Hill, New York, 2008.